



Neuronal synchronization enhanced by neuron–astrocyte interaction

Evgeniya V. Pankratova · Alena I. Kalyakulina · Sergey V. Stasenko · Susanna Yu. Gordleeva · Ivan A. Lazarevich · Viktor B. Kazantsev

Received: 26 November 2018 / Accepted: 7 May 2019 / Published online: 22 May 2019
© Springer Nature B.V. 2019

Abstract In this study, we consider the problem of signal processing in neuron–astrocyte networks where the intercellular communication is described on the basis of a tripartite synapse concept. This type of communication involves combined contributions of pre- and postsynaptic neuronal compartments and components of the surrounding astrocyte to the processes of information transmission. Astrocyte-mediated regulation of neuronal activity is considered through the analysis of the response changes in the classical Hodgkin–Huxley model driven by excitatory synaptic current. It is shown that the complicated astrocyte-dependent dynamics of this current can lead to non-trivial changes in individual postsynaptic neuronal activity and, hence, in the cooperative activation of neuronal groups linked by the “astrocyte-mediated bridge”.

Keywords Neuron–astrocyte communication · Synchronization · Filtering · Depression of neuronal firing · Gliotransmitter-induced resonant response

1 Introduction

Information about external world received by the animals from the environment through sensory transmission should be bound and processed by central nervous system. This highly complicated system coordinates all organism’s functions by coherent temporal activations of various neuronal networks. In such networks, a lot of synaptic information is received by neurons contacting with thousands of synaptic terminals. At the network level, input signals are integrated and processed to elaborate the output signal in the form of specific electrical signals known as action potentials that are conveyed by neuronal axon to another neuron of the network. Such integration is the consequence of intrinsic neuronal properties taking into account nonlinear input–output relationship and functional properties of neurons with the selective responsiveness to different input signals [1, 2]. At cellular and molecular levels, the signaling is defined by changes of the membrane currents and membrane potential variations, which represent the result of the expression of ligand- and voltage-gated membrane channels and indicate electrical excitability of the neurons [3]. Neuronal discharges caused by various external currents [4–8], and by synaptic currents formed by varied presynaptic background activity

The work was supported by the Ministry of Science and Higher Education of the Russian Federation (Project No. 14.Y26.31.0022).

E. V. Pankratova (✉) · A. I. Kalyakulina
Institute of Information Technologies, Mathematics and Mechanics, Lobachevsky State University of Nizhny Novgorod, Nizhny Novgorod, Russia
e-mail: pankratova@neuro.nnov.ru

S. V. Stasenko · S. Yu. Gordleeva · I. A. Lazarevich · V. B. Kazantsev
Center of Translational Technologies, Lobachevsky State University of Nizhny Novgorod, Nizhny Novgorod, Russia

[9–12] have been thoroughly studied via both experimental and theoretical approaches. Indeed, the neurons with their electrical excitability and capability of fast signal transmission through the network are the key players in providing brain information processing. However, during the last two decades many facts were found stating that another cell type, e.g., glial cells and, particularly, astrocytes, can participate in signal transmission and information processing at both cellular and network levels [13].

The astrocytes do not express sodium channels and, hence, cannot generate electrical excitation. For a long time, they were mostly considered as passive cells providing structural and metabolic support for neurons. Indeed, the astrocytes play relevant roles in the processes of the development and physiology of the brain. Providing neurons with nutrients and facilitating the post-traumatic repair and scarring processes are among the important functions of astrocytes.

However, recent findings have shown that astrocytes can play significant role in processing of synaptic information. Based on empirical results, new mathematical models for description of neuronal electrical activity modulation due to the effect of astrocytes have been proposed [14, 15]. Particularly, within the frame of such modeling the induction of seizure-like neuronal discharge for abnormal astrocytic glutamate degradation processes has been predicted [14]. From experiments, it follows that astrocytes can display selective responsiveness to specific synaptic inputs, which rely to calcium-based excitability and intrinsic properties giving nonlinear input–output relationships [16]. Moreover, it has been recently shown that astrocytes disruption by gliotoxins strongly effects the rhythmic network activity that has been demonstrated on brainstem respiratory [17] and spinal cord locomotor networks [18]. Calcium elevations in astrocytes induce the release of various gliotransmitters which can affect neuronal excitability and, therefore, reveal the ability of astrocytes to influence neuronal network functioning. Specifically, such influence can be provided by glutamate or by gamma-aminobutyric acid (GABA) released from astrocytes NMDA receptor-mediated slow inward currents or GABA receptor-mediated slow outward currents, respectively [19–23]. Diffusing in the surrounding extracellular space the gliotransmitters can further modulate the synaptic strength binding to specific receptors at both pre- and postsynaptic sides. Following the experimental facts, many computational

models have been developed taking into account neuron to astrocyte interactions in modeling the interneuronal communication [24–28].

Among the most exciting impacts of the astrocytes, one can mention their ability to coordinate the neuronal network activations [29–31]. Because of the fact that astrocyte is affected by a large number of synapses, the gliotransmission should also contribute in the effect of neuronal synchronization. Particularly, it was demonstrated in hippocampal network, where calcium elevations in astrocytes and subsequent glutamate release led to the synchronous excitation of clusters of pyramidal neurons [19, 20]. Imaging data from cultured hippocampal slices indicated that correlated activity of neurons at network level can be reduced due to calcium buffering in astrocytes, whereas uncaging of calcium in astrocytes could trigger synchronized activity in the neuronal population [32]. Thus, astrocyte signaling can contribute significantly in the maintenance of synchronized activity patterns in the hippocampal networks. Another experimental study on brain slices revealed that artificial increase in the gliotransmitter release yielded synchronized generation of extrasynaptic NMDAR-mediated slow inward currents [33]. Synchronous astrocytic activity was also found to be linked to the slow-wave activity [34] and to cortical state switching [35]. The latter property of neuron–astrocyte networks was also found in modeling work [36], where UP/DOWN state transitions were induced by gliotransmitter-mediated synaptic bistability. Thus, a large variety of experiments and simulations have been performed to discover principles of neuron–astrocyte communication and its effect on brain information processing.

In this study, we focus on the astrocyte participation in synchronization of its neighboring neurons due to release of two types of gliotransmitters. The paper is arranged as follows: In Sect. 2, the details of mathematical modeling of interneuronal communication in the presence of common astrocyte are described. In Sect. 3, the main dynamical features of the astrocyte glutamate and D-serine impacts on the synaptic transmission are presented within the frame of individual postsynaptic neuronal activity. In Sect. 4, the role of these gliotransmitters for both the output frequencies and synchronization of the outputs is examined for various frequencies of the Poisson inputs. The final section of the study is focused on discussion of the presented results and outlines the conclusions.

2 Neuron–astrocyte communication: mathematical modeling

To study the astrocytic-mediated changes of neural network dynamics, we consider recently developed computational model for bidirectional glutamate-mediated astrocytic regulation of synaptic transmission [37] and generalize it for a neuronal subnetwork with the cells coupled via a common astrocyte.

A schematic drawing of the considered intercellular communication is shown in Fig. 1. Communication of pre- and postsynaptic neuronal cells occurs by release of glutamate into synaptic cleft. Released glutamate is cleared by diffusion and uptake by astrocytic glutamate transporters on the postsynaptic terminal. Part of such glutamate could also spill out of the cleft, reach the neighboring astrocyte and trigger the release of various gliotransmitters (glutamate, adenosine triphosphate, D-serine and gamma-aminobutyric acid) release [38]. From experimental works, it is known that gliotransmitters can affect both the pre- and postsynaptic parts of neurons. In this study, the astrocyte ability to modulate the neural activity is considered through the change of concentrations of astrocytic glutamate and D-serine. Released astrocytic glutamate diffuses extrasynaptically and binds to presynaptic receptors (mGluRs or NMDARs) [39–41] which can modulate further glutamate release from the synapse by different mechanisms. Conditions where the astrocytic glutamate depresses neurotransmitter release were studied circumstantially, for example, in [42]. Astrocytic release of D-serine is critical for the activation of postsynaptic NMDA receptors and the development of synaptic long-term potentiation [43,44]. The contributions of both astrocytic glutamate-induced presynaptic depression and D-serine-induced postsynaptic enhancement, are taken into account in model described below.

2.1 Astrocyte-dependent presynaptic dynamics

We assume that the mean field amounts of neurotransmitters, X_i , that reach the astrocyte and lead to the release of amount Y_G of glutamate gliotransmitter within the synaptic connection with the i -th postsynaptic neuron, are described by the following equations [37]:

$$\begin{aligned} \frac{dX_i}{dt} &= -\alpha_X \left[X_i - k_0 (1 + \gamma_G Y_G) H_x \left(I_{pre}^{(i)} - 0.5 \right) \right], \\ \frac{dY_G}{dt} &= -\alpha_G \left\{ Y_G - \left[1 + \exp \left(-\frac{\sum_{i=1}^n X_i - \theta_G}{k_G} \right) \right]^{-1} \right\}, \\ I_{pre}^{(i)}(t) &= \begin{cases} 1, & \text{if } t_j < t < t_j + \tau, \\ 0, & \text{otherwise,} \end{cases} \end{aligned} \tag{1}$$

where $I_{pre}^{(i)}(t)$ is a pulse signal from the presynaptic cells, H_x is the Heaviside step function, t_j is the event occurrence time at one of the presynaptic terminals satisfying Poisson distribution with average frequency f_{in} and τ is the pulse duration, $\tau = 1$ ms, $k_0 = 2$ is the efficacy of the release, $\alpha_X = 0.1$ is the neurotransmitter clearance constant, $\alpha_G = 0.01$ is the clearance rate for glutamate, $\theta_G = 1.2$, $k_G = 0.1$. Note that, the parameter γ_G is negative (see [37] for details). In (1) and further, the parameter i defines the number of the considered postsynaptic neurons. From experimental data, it is known that its value can be rather large. But in this study, we focus on two cases only: for $i = 1$ we describe the main features of the considered model, and for $i = 2$ we present the peculiarities of the synchronous neuronal activity within the frame of neuron–astrocyte communication.

2.2 Astrocytic impact in alteration of EPSCs dynamics

Excitatory postsynaptic currents (EPSCs), $I_{EPSCs}^{(i)}$, are described by the following equations:

$$\begin{aligned} \frac{dI_{EPSCs}^{(i)}}{dt} &= \alpha_I \left(-I_{EPSCs}^{(i)} - A H_x \left(I_{pre}^{(i)} - 0.5 \right) \right), \\ \frac{dY_D}{dt} &= -\alpha_D \left\{ Y_D - \left[1 + \exp \left(-\frac{\sum_{i=1}^n X_i - \theta_D}{k_D} \right) \right]^{-1} \right\}, \end{aligned} \tag{2}$$

where $\alpha_I = 0.1$ is the rate constant and A is the amplitude. We assume that the amplitude of the EPSCs satisfies the probability distribution, $P(A)$, in the following form:

$$P(A) = \frac{2A}{b^2} \exp \left(-\frac{A^2}{b^2} \right), \tag{3}$$

where $b = b_0(1 + \gamma_D Y_D)$ is the scaling factor and Y_D is the concentration of D-serine released from the

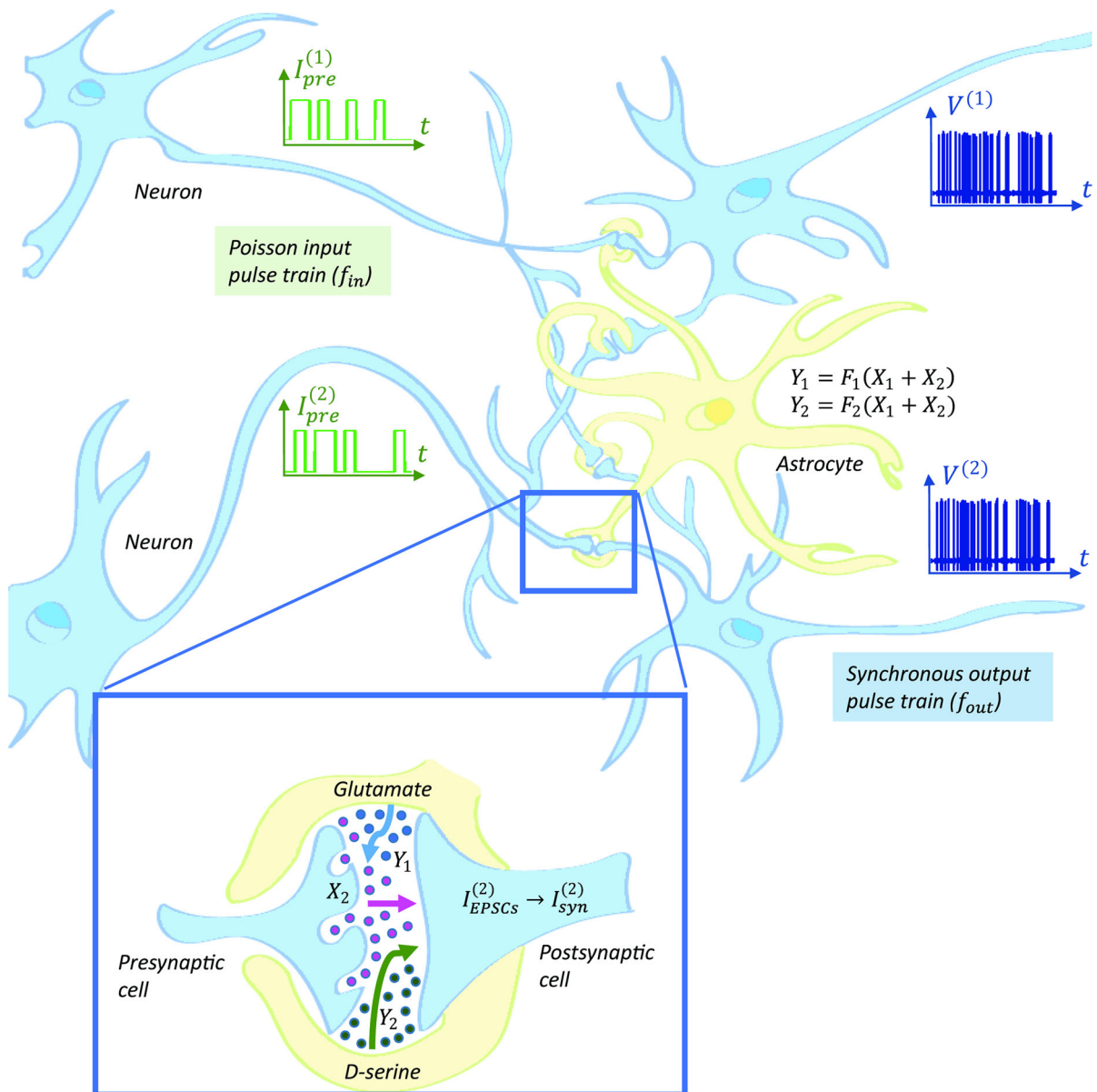


Fig. 1 Schematic sketch for astrocytic impact in interneuron communication

astrocyte. Note that, the parameter γ_D is positive. I_{syn} is the synaptic current, which is formed by integrating the postsynaptic events occurring at different sites. Because $I_{EPSCs}^{(i)}(t)$ is a mean field contribution of all synapses, I_{syn} can be expressed as

$$I_{syn}^{(i)} = I_{EPSCs}^{(i)} S_{\Sigma}, \tag{4}$$

where S_{Σ} is a dendrite integration function expressed here in the form of a high-pass filter:

$$S_{\Sigma} = \left[1 + \exp \left(- \left(\sum_{i=1}^n X_i - \theta_X \right) / k_X \right) \right]^{-1}, \tag{5}$$

where $\theta_X = 1.2$ and $k_X = 0.01$ are the midpoint and the slope of the neuronal activation, respectively. Midpoint and slope of gliotransmitter activation function are $\theta_D = 1.2$ and $k_D = 0.1$, respectively. The clearance constant of D-serine released from astrocyte is $\alpha_D = 0.01$.

2.3 Postsynaptic cells firing

The dynamics of postsynaptic cells is modeled by the basic Hodgkin–Huxley equations. The membrane potential is evolved according to the following current balance equation:

$$C \frac{dV_i}{dt} = I_{th} - I_{ion} - I_{syn}^{(i)}, \tag{6}$$

where $I_{ion} = I_{Na} + I_K + I_l$ is the sum of the transmembrane currents with

$$\begin{aligned} I_{Na} &= g_{Na} m_i^3(V_i) h_i(V_i) (V_i - E_{Na}), \\ I_K &= g_K n_i^4(V_i) (V_i - E_K), \\ I_l &= g_l (V_i - E_l) \end{aligned} \tag{7}$$

are the sodium I_{Na} and potassium I_K ionic currents passing through the cell membrane and the current I_l through an unspecific leakage channel, respectively.

The dynamics of the gating variables $n_i(V_i)$, $m_i(V_i)$, $h_i(V_i)$ is described by the following kinetic equations:

$$\begin{aligned} \frac{dn_i}{dt} &= \alpha_n(V_i)(1 - n_i) - \beta_n(V_i)n_i, \\ \frac{dm_i}{dt} &= \alpha_m(V_i)(1 - m_i) - \beta_m(V_i)m_i, \\ \frac{dh_i}{dt} &= \alpha_h(V_i)(1 - h_i) - \beta_h(V_i)h_i, \end{aligned} \tag{8}$$

where $m_i(V_i)$ and $h_i(V_i)$ are responsible for the activation and inactivation of the Na^+ -current, and $n_i(V_i)$ controls the K^+ -current activation. The mean transition rates of ionic channels from the closed to the open state, and vice versa, are described by the following functions:

$$\alpha_n(V_i) = \frac{0.01(V_i + 55)}{1 - \exp[0.1(-55 - V_i)]}, \tag{9}$$

$$\beta_n(V_i) = 0.125 \exp [(-V_i - 65)/80],$$

$$\alpha_m(V_i) = \frac{0.1(V_i + 40)}{1 - \exp[(0.1(-40 - V_i))]}, \tag{10}$$

$$\beta_m(V_i) = 4 \exp [(-V_i - 65)/18],$$

$$\begin{aligned} \alpha_h(V_i) &= 0.07 \exp[0.05(-V_i - 65)], \\ \beta_h(V_i) &= \{1 + \exp[0.1(-35 - V_i)]\}^{-1}. \end{aligned} \tag{11}$$

In (7), the parameters $g_{Na} = 120 \text{ mS/cm}^2$, $g_K = 36 \text{ mS/cm}^2$ and $g_l = 0.3 \text{ mS/cm}^2$ are the maximal conductances for the sodium, potassium and leakage channels, respectively, and $E_{Na} = 50 \text{ mV}$, $E_K = -77 \text{ mV}$ and

$E_l = -54.4 \text{ mV}$ are the corresponding reversal potentials. Note that, all the parameters were taken as in original work of A.L. Hodgkin and A.F. Huxley [45]. Only the reversal potentials and additive constants to V_i variable in functions $\alpha_k(V_i)$ and $\beta_k(V_i)$, $k = \{n, m, h\}$ were changed. Here, all values of the potentials were shifted on 65 mV because we focus on the time-dependent changes of the membrane potential while originally, the cell’s dynamics was studied for the displacement of the membrane potential from its resting value. The constant parameter introduced to Eq. (6) is $I_{th} = 5.7 \mu\text{A/cm}^2$.

Further, we numerically solved the described system by the fourth-order Runge–Kutta integration scheme with a time step of 0.001 ms. To avoid the influence of transients, the analysis of numerical data is carried out for $t > 500 \text{ ms}$. The mean output frequency value and the coefficient of synchronization (for the coupled postsynaptic neurons) were averaged over 200 different time series of postsynaptic membrane potential.

3 Astrocytic regulation of postsynaptic cell activity

3.1 Dynamics of the synaptic transmission

First, let us consider the dynamics of synaptic transmission. A pulse signal I_{pre} coming from the presynaptic cell triggers a series of reactions that evokes changing of the postsynaptic cell’s membrane potential in accordance with the following equations:

$$\begin{aligned} \frac{dX}{dt} &= -\alpha_X [X - k_0 (1 + \gamma_G Y_G) H_x (I_{pre} - 0.5)], \\ \frac{dY_G}{dt} &= -\alpha_G \{Y_G - [1 + \exp(- (X - \theta_G) / k_G)]^{-1}\}, \\ \frac{dI_{EPSCs}}{dt} &= -\alpha_I (I_{EPSCs} + A H_x (I_{pre} - 0.5)), \\ \frac{dY_D}{dt} &= -\alpha_D \{Y_D - [1 + \exp(- (X - \theta_D) / k_D)]^{-1}\}, \\ C \frac{dV}{dt} &= I_{th} - I_{ion} - I_{EPSCs} [1 + \exp(- (X - \theta_X) / k_X)]^{-1}, \end{aligned} \tag{12}$$

where the equations describing the dynamics of the gating variables are omitted for simplicity. The parameter A is a random amplitude satisfying the probability distribution (3) with $b = b_0(1 + \gamma_D Y_D)$, and b_0 is the scaling factor accounting for the strength of the synaptic response on stimulation. The efficacy of neurotransmitter release $k_0 = 2$ is assumed to be constant.

For illustration, we fix most of the parameters with constant values and focus on the effect of some of them only. Note that, here, for the cell-to-cell astrocyte-mediated communication through a single synaptic cleft, we consider the midpoints of the functions used for detection of neurotransmitters impact on gliotransmitters concentration and synaptic current as $\theta_G = \theta_D = \theta_X = 0.7$. All another parameters are taken as in Sect. 2. As was mentioned before, the parameters γ_G and γ_D have been introduced to the model for accounting the gain of astrocytic glutamate and D-serine. Thus, the main features appeared due to the change of these parameters will be discussed in detail further on.

In Fig. 2a, from top to bottom we present two examples for time evolution of the input signal I_{pre} , the mean field amount of neurotransmitter X released from the presynaptic terminal, the mean field contribution into the change of EPSC currents (I_{EPSCs}) on a patch of postsynaptic membrane and, finally, the postsynaptic cell's membrane potential change $V(t)$. Blue data were obtained for input signal I_{pre} with $f_{\text{in}} = 300$ p/s and scaling factor of EPSCs amplitudes' distribution $b_0 = 10$. Note that, the choice $b_0 = 10$ corresponds to EPSCs amplitudes distributed near the value $A = b_0/\sqrt{2} \approx 7.07 \mu\text{A}/\text{cm}^2$.

While the duration of each pulse in the input signal I_{pre} has been fixed ($\tau = 1$ ms), the Poisson pulse train for high frequencies f_{in} can exhibit the pulses with a longer duration (see the magnified part in the inset in Fig. 2a). This can be explained as follows. In accordance with the probability distribution for the intervals τ_{in} shown in Fig. 2b, for $f_{\text{in}} = 300$ p/s the probability for appearance of zero-value becomes rather large. Within the frame of the model, this situation is considered as the appearance of synchronized pulse events whose duration becomes larger. Such high frequency stimulation significantly increases the mean field amount of neurotransmitters X diffusing into the synaptic cleft. Red line depicted for $X = 0.7$, defines the midpoint of astrocyte activation function $[1 + \exp(-(X - \theta_{G,D})/k_{G,D})]^{-1}$. For X exceeding this threshold, the values of Y_G and Y_D variables are increased (not shown) and for nonzero values of parameters γ_G and γ_D this leads to a gain of astrocytic glutamate and D-serine impacts on the postsynaptic dynamics. Particularly, for $\gamma_G = 0$ and $\gamma_D = 1$, due to such exceeding effect, the membrane potential change $V(t)$ in the presence of high-frequency stimulation demonstrates the appearance of the spikes in postsynaptic

cell's response. On the contrary, for low-frequency input signals, the interpulse intervals in I_{pre} become large (the probability distribution of interpulse durations in I_{pre} for $f_{\text{in}} = 100$ p/s is shown in Fig. 2b by green color) and the concentration of the released neurotransmitter is weakly changed in time. This leads to small oscillations of both X and I_{EPSCs} and, therefore, cannot evoke any postsynaptic cell's response (green data in $V(t)$ -dependence).

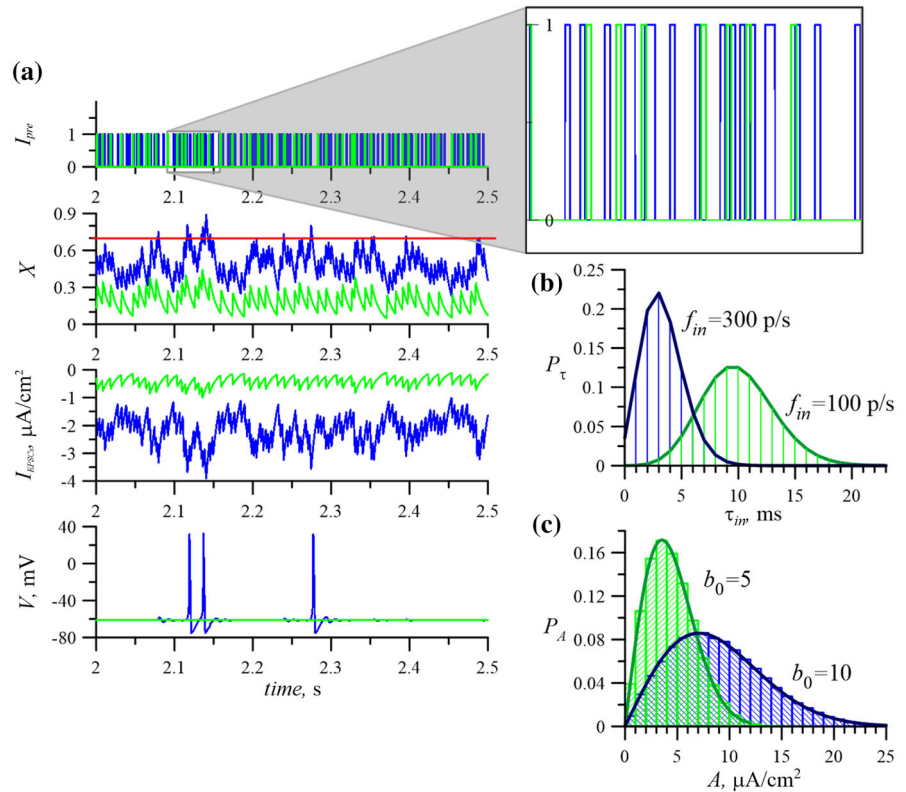
3.2 Potentiating and depressing effects on neuronal response

From experimental works, it is known that astrocyte-released glutamate leads to presynaptic depression [42] while the release of D-serine evokes the postsynaptic enhancement of the neuron's response. Recently developed model of neuron-astrocyte interaction, taking into account the changes of mean field amounts of neurotransmitter and gliotransmitters release [37], permits describing both these effects.

In order to illustrate the peculiarities of astrocytic regulation within the frame of the system (12), we present two time series of the postsynaptic cell's membrane potential $V(t)$ calculated for $\gamma_D = 0$ and $\gamma_D = 5$ (see Fig. 3a, b, respectively). As can be seen from these numerical data, the increase in postsynaptic upscaling leads to the increase in the spike generation frequency.

To show the details of the astrocyte-mediated output change, we calculate the durations of the interspike intervals for γ_G varied from -5 to 0 (assuming that $\gamma_D = 0$) and for γ_D varied from 0 to 5 (for the fixed gain of presynaptic depression $\gamma_G = 0$). To plot the diagram shown in Fig. 3c, for each value of γ_G and γ_D the time of integration has been varied to obtain the same number ($n = 500$) of spikes generated by the postsynaptic cell. It follows from Fig. 3c that for all values of parameters γ_G and γ_D the smallest interval duration is ≈ 0.017 s. This duration is defined by the existence of refractory period that starts immediately after the excitation and during which a neuron is unresponsive to further stimulation (see the inset in Fig. 3a for detail). The histograms calculated for various values of γ_G and γ_D (not shown) reveal that this interspike interval is the most frequently appeared event in cell's output. This is due to the fact of appearance of the so-called short-ISI spikes (see the inset in Fig. 3a). This type of response

Fig. 2 a From top to bottom: time series of presynaptic events I_{pre} in the form of Poisson pulse train (with enlarged part in the inset); the mean field concentration of neurotransmitter X ; the mean field postsynaptic current I_{EPSCs} and the membrane potential changes of the postsynaptic cell. The data shown in blue color were obtained for $f_{in} = 300$ p/s and $b_0 = 10$, and green color is for $f_{in} = 100$ p/s and $b_0 = 5$. Red line for $X = 0.7$ depicts the threshold defining the conditions for spike generation. The parameters of gliotransmitters release gain are $\gamma_G = 0$ and $\gamma_D = 1$. Probability distributions for the intervals between pulses in I_{pre} and for the amplitudes of EPSCs are presented in **b** and **c**, respectively. (Color figure online)



is frequently measured in various biological studies. Recent results in this field suggest that burst-like firing should be more efficient in signal transmission and could convey more information per spike than the firing containing another ISI subsets [46,47]. From the point of view of the considered model, the existence of such short-ISI spikes is provided by the form of the synaptic current I_{syn} . It has mostly smoothed shape of a rectangular-type pulse whose width allows generation of several consecutive spikes. Since the gain of presynaptic depression γ_G leads to constriction of I_{syn} shape, the generation of short-ISI spikes in this case does not occur. In the inset in Fig. 3c, the narrow subregion corresponding to the smallest interspike duration for large γ_G disappears.

On the other hand, large interspike intervals in cell's output form wide subregion with high distribution density for smaller intervals and, on the contrary, low density for the larger intervals. Wherein for large γ_D long-length interval durations tend to disappear, the number of short-ISI spikes and their mean length (i.e., the number of spikes within this burst-like firing) are increased.

Therefore, the depressing ability of glutamate on neurotransmitters release leads to the significant decrease in the output frequency of postsynaptic firing, while the gain of the released D-serine enhances the response. Figure 4 (curves to the left of f_{out} -axis) shows that large enough increase in γ_G can suppress the neuronal response at all. For any I_{pre} stimulation some amount of astrocyte-released glutamate γ_G^* exists that for $\gamma_G > \gamma_G^*$ (in absolute values) the postsynaptic cell falls into a quiescent mode.

On the contrary, the increase in γ_D corresponding to the gain of the D-serine-mediated influence, leads to increase in the output frequency, as shown in Fig. 4 (curves to the right of f_{out} -axis).

3.3 Frequency filtering

Postsynaptic cell's membrane potential calculations for various values of frequencies f_{in} of the input signal I_{pre} show that for high values of f_{in} , almost tonic spiking is observed. Contrary, for small f_{in} most of the spikes are suppressed, and for instance, at $f_{in} = 100$ p/s only few spikes are generated. Thus, the system can be consid-

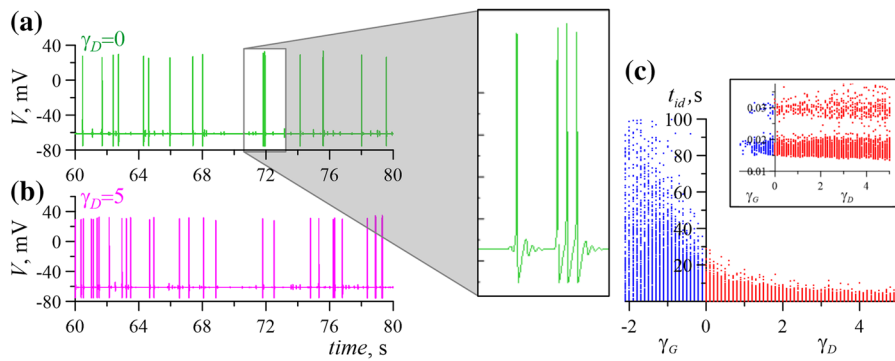


Fig. 3 Time traces of the postsynaptic membrane potential $V(t)$ at different concentrations of the released D-serine: **a** $\gamma_D = 0$ and **b** $\gamma_D = 5$. The inset shows an enlarged part of the neuronal response in the form of short-ISI spikes. **c** Interspike intervals distribution for various concentrations of astrocytic glutamate (blue

dots) and D-serine (red dots). The inset shows dense distribution of the shortest intervals defined by the existence of neuronal refractory period. The parameters are the frequency of the Poisson input is $f_{in} = 300$ pulses per second, $b_0 = 5$, $\theta_X = 0.7$. (Color figure online)

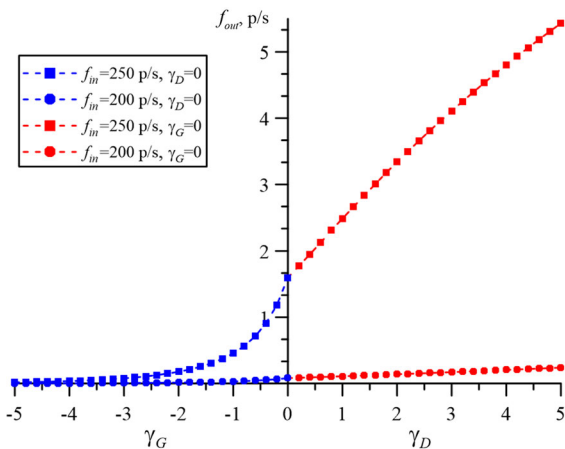


Fig. 4 The dependence of the output frequency on the gain of presynaptic feedback γ_G and postsynaptic upscaling γ_D for two values of the Poisson input frequency f_{in} , $b_0 = 5$, $\theta_X = 0.7$

ered as a high-pass filter whose cutoff frequency f_c can be altered due to astrocytic influence. Both astrocytic glutamate and D-serine release change the cutoff frequency: the increase in D-serine concentration leads to a decrease in f_c , while the gain of glutamate increases the cutoff frequency, as shown in Fig. 5.

For the considered set of parameters, the role of D-serine in modulation of the cutoff frequency is not so well pronounced and does not exceed 1% in comparison with the case $\gamma_G = \gamma_D = 0$, while the gain of astrocytic glutamate provides more than 20% increase of the cutoff frequency. Indeed, from [37] it is known

that the highest impact of γ_G is observed for low input frequencies, while the role of γ_D is more significant for higher values of f_{in} .

Further, we will show how these dynamical features do impact on postsynaptic cells synchronization.

4 Neuronal activity caused by common astrocytic modulation of synaptic transmission

To quantify the interrelation of spiking events for the coupled postsynaptic cells, we consider a measure that can be deduced from raster diagrams data widely used in experimental neuroscience. This is the *coefficient of synchronization* that for two neurons can be defined by the following relation:

$$\eta = \frac{2n_{sync}}{n_1 + n_2}, \tag{13}$$

where n_1 and n_2 are the numbers of spikes produced by the first and by the second postsynaptic cells, respectively. The number of synchronous spikes is denoted as n_{sync} . Obviously, that for synchronous firing of the postsynaptic cells $\eta = 1$, and for asynchronous generation $\eta = 0$. It should be noted that due to nonidentity of the driving (the currents $I_{syn}^{(i)}$ are varied from cell to cell), the complete synchronization of spikes cannot be expected. Therefore, in the following, we assume that two spiking events can be considered as synchronous if the membrane potentials of both cells exceed the value

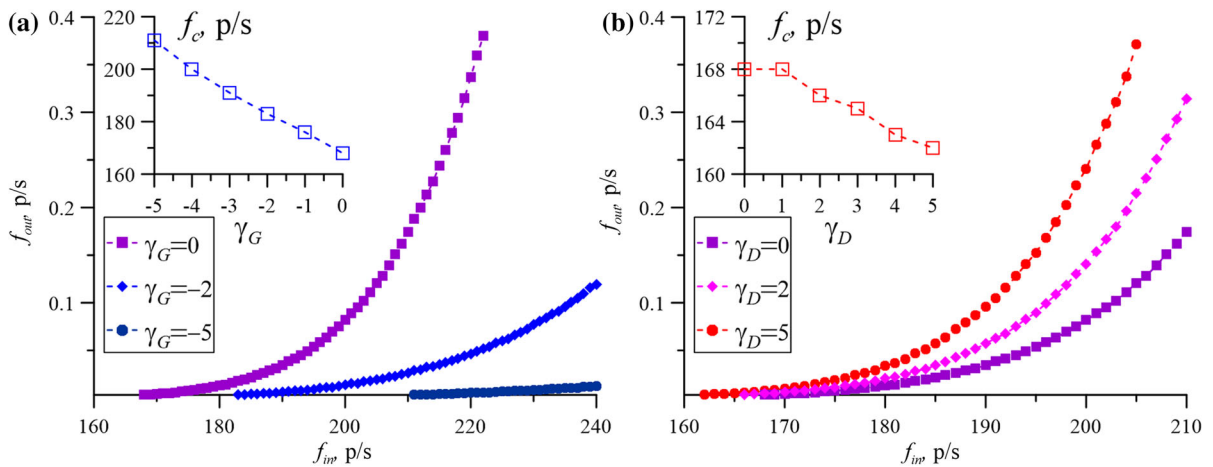


Fig. 5 Output frequency dependence on f_{in} for three values of **a** γ_G and **b** γ_D . In the insets: the cutoff frequency changes with the increase in γ_G and γ_D , respectively. The parameters are $b_0 = 5$, $\theta_X = 0.7$

of $V_{th} = -40$ mV. Taking into account an average width of the spike at the level of V_{th} , this assumption corresponds to consideration of 2-ms-timing window for registration of synchronous events.

Since the change of gliotransmitters amount significantly impacts on the output frequency, we also calculate the mean frequency of the neuronal postsynaptic firing as $f_{out} = (f_{out}^{(1)} + f_{out}^{(2)})/2$.

4.1 Neuronal output synchronization

Without astrocytic-mediated modulations, the considered neuronal communication occurs through a synapse that uses glutamate as the transmitter, and that has receptors opening channels for cations. When these glutamate receptors are activated, both Na^+ and K^+ flow across the membrane of postsynaptic neuron. If temporary depolarization of postsynaptic membrane caused by this flow changes the membrane potential so that it exceeds threshold, the postsynaptic neuron will produce an action potential. In general case, the strength of the EPSCs does not have any constant value. A lot of factors influence its amplitude. Since a neuron may receive the information from many synaptic inputs with other neurons, in the considered model, the variable I_{EPSCs} is considered as the mean field contribution of all synapses. In simulations, the strength of excitatory postsynaptic current caused by all incoming stimuli, is defined by the parameter b_0 . Therefore, the synchronization features will further be discussed for

two possible cases, namely for weak and strong EPSCs, i.e., for small and large values of b_0 .

4.1.1 Gliotransmitters impact for strong EPSCs

Here, the EPSCs are assumed to be strong if the considered band of astrocytic-mediated modulations do not suppress the response of postsynaptic neurons, i.e., for any considered γ_G and γ_D , the frequency of postsynaptic firing f_{out} does not take zero values. For convenience, we start with the case when the gliotransmitters impact on neuronal dynamics separately. In particular, the gain of presynaptic depression is studied in the absence of postsynaptic modulations ($\gamma_D = 0$) and conversely, for varying γ_D we assume that $\gamma_G = 0$. Since the role of the input frequency of the Poisson stimulation is of significance [37], we focus on both low- and high-frequency cases.

Uncooperative role of gliotransmitters release for low input frequencies. Figure 6a–d shows the raster diagrams for four combinations of γ_G and γ_D parameters: (a) and (b) were obtained for varying γ_D and (c) and (d) present the results for two values of γ_G ($\gamma_D = 0$). These diagrams were obtained numerically for $b_0 = 10$ and for Poisson inputs with $f_{in} = 250$ pulses per second. To characterize the response, we calculate the dependence of output frequency f_{out} and coefficient of synchronization η on γ_G and γ_D as illustrated in Fig. 6e, f. Thus, the highest degree of the neuronal synchronization is observed for $\gamma_G = 0$, $\gamma_D = 5$ where

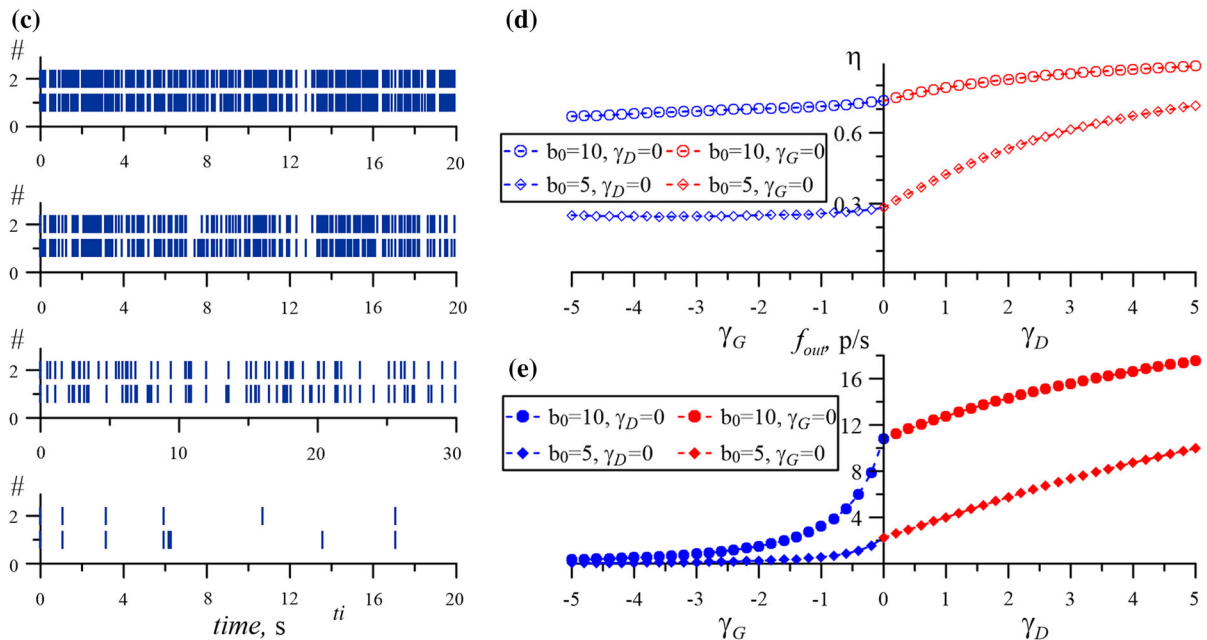


Fig. 6 Raster diagrams obtained for four combinations of γ_G and γ_D : **a** (0, 5), **b** (0, 0), **c** (-1.5, 0) and **d** (-5, 0). **e** The dependence of synchronization coefficient η on both γ_G and γ_D for $b_0 = 10$ is shown by empty blue (left part of the curve) and red (right part of the curve) circles, respectively; for $b_0 = 5$ —by empty diamonds. Blue and red filled circles in **f** correspond

to the changes for $b_0 = 10$ of the output frequency with the gain of presynaptic depression $-\gamma_G$ (left part of the curve) and with the gain of the D-serine effect γ_D (right part of the curve), respectively; filled diamonds are for $b_0 = 5$. The parameters are $f_{in} = 250$ p/s, $\theta_X = 1.2$. (Color figure online)

the high-frequency generation with 85% coincidence of spikes occurs. It follows from Fig. 6e that the considered gain of D-serine release leads to approximately 60% increase of the output frequency and 20% increase of η . On the contrary, the growth of astrocytic glutamate leads to significant decrease in f_{out} (up to 95%), but η changes weakly due to this γ_G -decrease and its change does not exceed 8%.

Taking the smaller values of b_0 , the larger increase in synchronization with the increase in γ_D is observed (for instance, for $b_0 = 5$, more than double increase in η occurs). At the same time, the changes of γ_G have weak impact on η within the considered band of values. Summarizing the results obtained for low input frequencies, it becomes clear that the growth of D-serine release monotonically enhances the postsynaptic cell's response and increases the ability for postsynaptic cells' synchronization. The increase in astrocytic glutamate release, on the contrary, leads to inhibition of the response with slightly changing the coefficient of synchronization.

Uncooperative role of gliotransmitters release for high input frequencies. As for the low frequencies, the highest ability to synchronize the neuronal outputs is observed for the largest values of b_0 . Particularly, for $b_0 = 10$, η (that becomes larger for all values of γ_G and γ_D in comparison with the low-frequency case) with the increase in γ_D converges to 0.98 illustrating the improvement of synchronization up to the level of almost completely synchronous firing of the postsynaptic cells. As in Fig. 6e, for extremely strong EPSCs either monotonic amplification (with the increase in γ_D) or monotonic attenuation (with the increase in $-\gamma_G$) of η occurs depending on the type of gliotransmitter released (see Fig. 7a for comparison).

For smaller amplitudes of EPSCs, the dependencies of both f_{out} and η on presynaptic depression (i.e. on γ_G) demonstrate a non-trivial behavior. Despite the monotonic decrease in the released amount of presynaptic neurotransmitters X , both f_{out} and η have maximum at the certain value of γ_G . Particularly, for $b_0 = 5$, γ_G -induced η -amplification is 26% whereas the out-

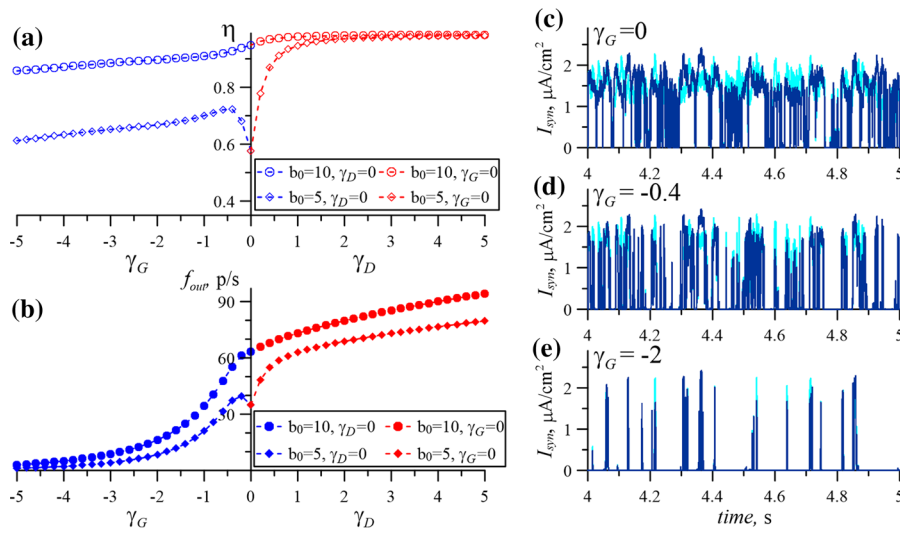


Fig. 7 **a** Coefficient of synchronization η versus both γ_G (blue empty symbols at the left part of the curve) and γ_D (red empty symbols at the right part of the curve) for two values of b_0 : $b_0 = 5$ (diamonds) and $b_0 = 10$ (circles). Filled symbols in **b** represent the output frequency as function of γ_G (blue symbols) and γ_D

(red symbols) for $b_0 = 5$ (diamonds) and $b_0 = 10$ (circles). Time series of synaptic currents I_{syn} that are supplied to the neurons for three values of γ_G : **c** $\gamma_G = 0$, **d** $\gamma_G = -0.4$ and **e** $\gamma_G = -2$. The parameters are the mean frequency of both Poisson inputs are $f_{in} = 500$ pulses per second, $\theta_X = 1.2$. (Color figure online)

put frequency demonstrates more than 30% increase in comparison with the case of $\gamma_G = 0$. So that, for high frequencies of the Poisson signal the response enhancement is possible due to changes of both presynaptic depression and postsynaptic upscaling.

To explain the appearance of non-monotonic dependence of f_{out} and η on presynaptic depression, further we describe the conditions for spike generation in Hodgkin–Huxley model subjected to two types of input signals.

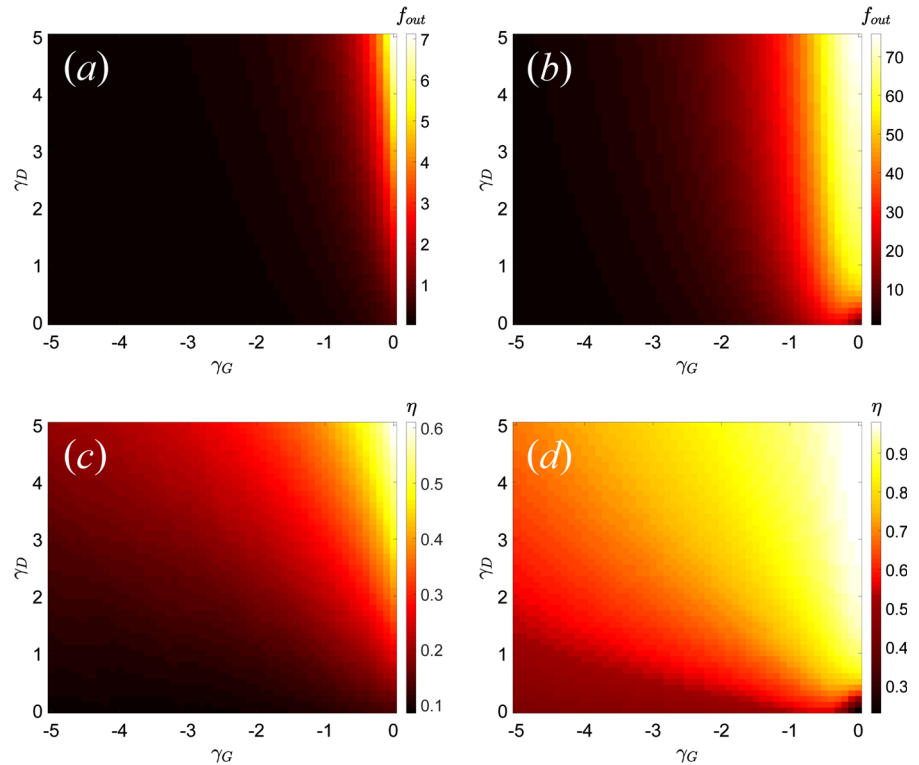
Role of input currents in emergence of tonic firing in Hodgkin–Huxley model. Tonic neuronal activity is characterized by stable action potential firing at constant frequency. Such type of behavior can be observed as a result of sufficiently large intensities of external stimulation. The most well-known cases of such stimulations are the dc- and ac-currents. The role of the parameters of these injections is of particular importance and was circumstantially studied both experimentally [4] and through various simulations [5–8].

For dc-current, the classical Hodgkin–Huxley model describes two types of behavior: quiescent state or periodic firing. The unique stable equilibrium state corresponding to the first one, is observed for amplitudes of current not exceeding $I_{dc}^{(1)} \approx 6.2 \mu A/cm^2$. The

unique stable limit cycle \mathcal{L}^s corresponding to the firing regime, exists for $I_{dc} > I_{dc}^{(2)} \approx 9.8 \mu A/cm^2$ until some extremely large value of I_{dc} that is not reached in this study. Within the interval $I_{dc}^{(1)} < I_{dc} < I_{dc}^{(2)}$ both stable equilibrium state and stable limit cycle coexist in the phase space of the dynamical system. It should be noted that the equilibrium state loses the stability at $I_{dc} = I_{dc}^{(2)}$ through the subcritical Andronov–Hopf bifurcation resulting in emergence of an unstable limit cycle \mathcal{L}^u for $I_{dc} < I_{dc}^{(2)}$, whereas the stable limit cycle \mathcal{L}^s merging with \mathcal{L}^u disappears through the saddle-node bifurcation of periodic orbits at $I_{dc} = I_{dc}^{(1)}$. It is important that the increase in I_{dc} within the range of bistability leads to an increase in the output frequency from approximately 52–70 Hz [6].

For ac-current, in Hodgkin–Huxley model, besides a non-firing state various regimes of regular and irregular oscillations depending on the amplitude and frequency of the applied current are possible. Particularly, in [7,8] it has been shown that signals with amplitudes smaller than $I_{ac} \approx 1.6 \mu A/cm^2$ cannot evoke a response for any driving frequency. And for amplitudes smaller than $I_{ac} \approx 2.5 \mu A/cm^2$ only various types of regular oscillations are possible. Irregular responses as well as the so-called 3 : 1 lockings

Fig. 8 The output frequency f_{out} and synchronization coefficient η vs γ_G and γ_D for **a, c** $f_{in} = 250$ p/s and **b, d** $f_{in} = 500$ p/s. The parameters are $b_0 = 4$, $\theta_X = 1.2$



(that corresponds to the response with one spike per 3 stimulus cycles) occur only for larger amplitudes, for $I_{ac} > 2.5 \mu\text{A}/\text{cm}^2$ and $I_{ac} > 3.5 \mu\text{A}/\text{cm}^2$, respectively. Moreover, it is worth noticing that this variety of oscillatory regimes observed for $I_{ac} < I_{dc}^{(1)}$, is possible only within the bounded range of input frequencies: there is no response in Hodgkin–Huxley model for low and high frequencies of ac-current.

Therefore, the comparison of the thresholds for dc- and ac-currents reveals that frequency-dependent component in input signal can significantly reduce the threshold for spike generation and, consequently, enhance the postsynaptic cells response.

In Fig. 7c–e, modulations of the synaptic currents $I_{syn}^{(1,2)}$ due to the increase in the astrocytic glutamate are presented. One can note that the maximal amplitude of this signal is not changed while the frequency changes significantly. Note that, such frequency-induced enhancement can be observed only due to the change of γ_G . Moreover, for smaller values of b_0 the larger enhancement of the neuronal response is observed. Particularly, for $b_0 = 4$, more than double amplification of η due to the increase in astrocytic glutamate is observed (not shown).

Joint impact of presynaptic depression and postsynaptic upscaling. To study the synchronizing influence of the common driving $I_{syn}^{(i)}$ applied to the postsynaptic cells for arbitrary varied amounts of the gliotransmitters released, we present the division of the parameter plane (γ_G , γ_D) into the regions with different types of cells response. The lighter domains in Fig. 8a, b correspond to the regimes of postsynaptic firing where the output frequency becomes high. For this regime the number of synchronous spikes and, correspondingly, η both take their maximal values. The darker domain in Fig. 8c depicts the regimes of low-frequency firing with less than 15% coincidence of spikes in the postsynaptic cells responses.

4.1.2 Gliotransmitters impact for weak EPSCs

For weak EPSCs, the change of gliotransmitters release decreasing the neuron's response can also completely suppress it. To show this, we consider two values of the parameter b_0 : $b_0 = 2.5$ and $b_0 = 3.5$ for the same value of the input Poisson signal frequency $f_{in} = 200$ pulses per second. For these cases, the dependencies of response on both η and f_{out} are presented in Fig. 9a, b.

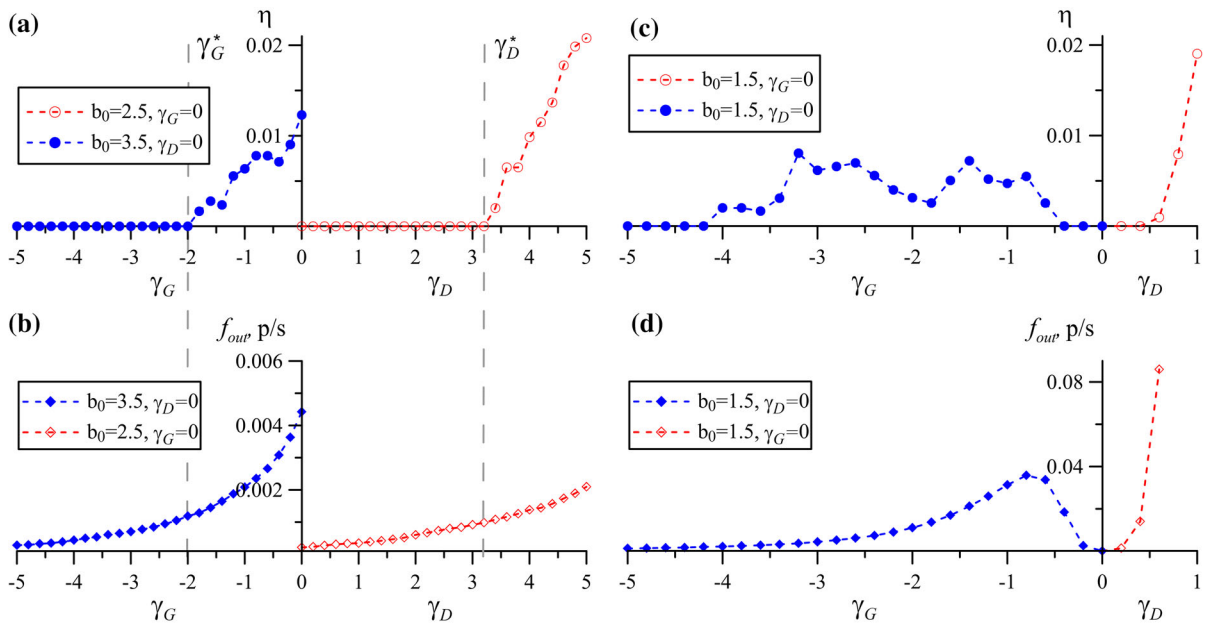


Fig. 9 In **a** and **c** the dependence of synchronization coefficient η on both γ_G and γ_D is shown by blue filled and red empty circles, respectively. Blue filled and red empty diamonds in **b** and **d** correspond to the changes of the output frequency with the

change of γ_G and γ_D , respectively. The parameters are the mean frequency of a Poisson input I_{pre} is $f_{in} = 200$ pulses per second, $\theta_X = 1.2$. In **a** and **b** $b_0 = 2.5$ and $b_0 = 3.5$; in **c** and **d** $b_0 = 1.5$, $f_{in} = 500$ pulses per second. (Color figure online)

One can see that depending on the value of b_0 either γ_G^* or γ_D^* -threshold for the appearance of the cells synfire activity exists. Taking into account the effects of gliotransmitters on the dynamics of the postsynaptic cell, the increase in η is much faster for the synfire activity emerged through the exceeding of some γ_D^* -threshold.

For high input frequencies, due to the previously described resonant effect two γ_G^* -thresholds can be observed with the change of γ_G , Fig. 9c, d.

5 Discussion

Any information sent to the central nervous system is transmitted through the correlated changes of the membrane potentials in certain temporary activated groups of neurons. The role of the driving characteristics in the collective dynamics of these neuronal subnetworks is of particular interest. The most studies in this field were carried out within the frame of homogeneous networks of neurons [48–58]. The last knowledge of astrocyte dynamics and neuron–astrocyte interactions indicates that most of traditional models used for description of intercellular communication need to be modified [59].

Indeed, the development of fluorescent imaging techniques permitted to demonstrate that astrocytes should be true members of information processing game in the central nervous system. Specifically, they can dynamically shape the extracellular space and exert a regulatory influence on the neuronal signaling by affecting the extracellular diffusion of neurotransmitters [60,61]. Astrocytes can control the extracellular K^+ concentration through the expression of specific ion channels. An expression of these channels has been proposed to contribute to neuronal hyperexcitability and epilepsy [62]. It was shown, that expression of glutamate transporters by astrocytes is crucial in the clearance of glutamate from the synaptic cleft to terminate synaptic function [63]. Transmitter transporter dysfunctions can lead to pathological conditions, including neuronal networks hyperexcitability and epileptic activity development [64].

In this study, based on earlier developed model for the tripartite synapse [37] we addressed non-trivial changes in coherence and synchronization of neuronal activity induced by the gliotransmitter release.

We have assumed that the dynamics of postsynaptic neurons is described by the basic Hodgkin–Huxley model forced by synaptic currents. The dynamics of these currents depends both on the concentration of neurotransmitter released by the presynaptic neuron (responding on the incoming stimulation in the form of the Poisson pulse train) and the concentration of D-serine released by the astrocyte, whereas the change of neurotransmitter amount within the synaptic cleft depends both on incoming signal (the Poisson pulse train) and the concentration of astrocytic glutamate. It is assumed that astrocytic glutamate depresses the presynaptic release while D-serine enhances the postsynaptic currents. For low-frequency inputs, the monotonic glutamate-induced depression and D-serine-induced potentiation of the postsynaptic neuronal activity are observed. On the contrary, for high-frequency inputs, the joint effect of high-frequency-induced increase in neurotransmitter concentration and its decrease due to the increase in astrocytic glutamate, leads to non-monotonic change of the neuronal response. It has been shown that astrocyte-mediated presynaptic depression for incoming high-frequency stimulation can provoke a *resonant neuronal response* and, hence, lead to significant increase in the output frequency.

We have also examined the astrocyte feature to influence on the degree of the output synchronization. Since the Poisson inputs are not synchronized (only the mean input frequencies are assumed to be constant), the synaptic currents driving the postsynaptic cells are not identical. Correspondingly, the complete synchronization (i.e. the complete coincidence of the membrane potentials V_i) is not possible in this case. To quantify this dynamics, we propose a specific measure called *coefficient of synchronization*. Calculation of this coefficient reveals the significant contribution of gliotransmitters to modulation of the neuronal activity. For high-frequency inputs, apart from the response enhancement, the degree of synchronization is also significantly increased.

Recently detected physiological consequences of the communication between astrocytes and neurons reveal a lot of non-trivial facts. The current knowledge about this intercellular communication is mostly the result of investigations at the cellular and molecular levels. Despite the numerous models for the description of signal transmission via tripartite synapses, the heterogeneous networks of cells as the higher level of complexity and the actual impact of astrocytes in the

neuronal network activity are still the subject of further detailed simulation studies.

Acknowledgements The numerical computations were carried out on high-performance cluster of Lobachevsky State University of Nizhny Novgorod.

Compliance with ethical standards

Conflict of interest The authors declare that they have no conflict of interest.

References

1. Llinas, R., Sugimori, M.: Electrophysiological properties of in vitro Purkinje cell dendrites in mammalian cerebellar slices. *J. Physiol.* **305**, 197–213 (1980)
2. Agmon-Snir, H., Carr, C.E., Rinzel, J.: The role of dendrites in auditory coincidence detection. *Nature* **393**, 268–272 (1998)
3. Hille, B.: *Ion Channels of Excitable Membranes*. Sinauer Associates, Sunderland (2001)
4. Matsumoto, G., Aihara, K., Hanyu, Y., Takahashi, N., Yoshizawa, S., Nagumo, J.: Chaos and phase locking in normal squid axons. *Phys. Lett. A* **123**, 162–166 (1987)
5. Parmananda, P., Mena, C.H., Baier, G.: Resonant forcing of a silent Hodgkin–Huxley neuron. *Phys. Rev. E* **66**, 047202 (2002)
6. Lee, S.-G., Neiman, A., Kim, S.: Coherence resonance in a Hodgkin–Huxley neuron. *Phys. Rev. E* **57**(3), 3292–3297 (1998)
7. Pankratova, E.V., Polovinkin, A.V., Mosekilde, E.: Resonant activation in a stochastic Hodgkin–Huxley model: interplay between noise and suprathreshold driving effects. *Eur. Phys. J. B* **45**(3), 391–397 (2005)
8. Pankratova, E.V., Belykh, V.N., Mosekilde, E.: Role of the driving frequency in a randomly perturbed Hodgkin–Huxley neuron with suprathreshold forcing. *Eur. Phys. J. B* **53**(4), 529–536 (2006)
9. Tsodyks, M.V., Markram, H.: The neural code between neocortical pyramidal neurons depends on neurotransmitter release probability. *PNAS* **94**(2), 719–723 (1997)
10. Uzuntarla, M.: Inverse stochastic resonance induced by synaptic background activity with unreliable synapses. *Phys. Lett. A* **377**(38), 2585–2589 (2013)
11. Uzuntarla, M., Ozer, M., Ileri, U., Calim, A., Torres, J.J.: Effects of dynamic synapses on noise-delayed response latency of a single neuron. *Phys. Rev. E* **92**(6), 062710 (2015)
12. Uzuntarla, M., Torres, J.J., So, P., Ozer, M., Barreto, E.: Double inverse stochastic resonance with dynamic synapses. *Phys. Rev. E* **95**, 012404 (2017)
13. Verkhratsky, A., Butt, A.: *Glial Neurobiology. A Textbook*, 1st edn, p. 224. Wiley, Hoboken (2007)
14. Li, J., Tang, J., Ma, J., Du, M., Wang, R., Wu, Y.: Dynamic transition of neuronal firing induced by abnormal astrocytic glutamate oscillation. *Sci. Rep.* **6**, 32343 (2016)

15. Guo, S., Tang, J., Ma, J., Wang, C.: Autaptic modulation of electrical activity in a network of neuron-coupled astrocyte. *Complexity* **2017**, 4631602 (2017)
16. Araque, A.: Astrocytes process synaptic information. *Neuron Glia Biol.* **4**, 3–10 (2008)
17. Hülsmann, S., Oku, Y., Zhang, W., Richter, D.W.: Metabolic coupling between glia and neurons is necessary for maintaining respiratory activity in transverse medullary slices of neonatal mouse. *Eur. J. Neurosci.* **12**, 856–862 (2000)
18. Baudoux, S., Parker, D.: Glial-toxin-mediated disruption of spinal cord locomotor network function and its modulation by 5-HT. *Neuroscience* **153**, 1332–1343 (2008)
19. Angulo, M.C., Kozlov, A.S., Charpak, S., Audina, E.: Glutamate released from glial cells synchronizes neuronal activity in the hippocampus. *J. Neurosci.* **24**, 6920–6927 (2004)
20. Fellin, T., Halassa, M.M., Terunuma, M., Succol, F., Takano, H., Frank, M., Moss, S.J., Haydon, P.G.: Endogenous non-neuronal modulators of synaptic transmission control cortical slow oscillations in vivo. *Proc. Natl. Acad. Sci. USA* **106**, 15037–15042 (2009)
21. Perea, G., Araque, A.: Properties of synaptically evoked astrocyte calcium signal reveal synaptic information processing by astrocytes. *J. Neurosci.* **25**, 2192–2203 (2005)
22. Kozlov, A.S., Angulo, M.C., Audinat, E., Charpak, S.: Target cell-specific modulation of neuronal activity by astrocytes. *Proc. Natl. Acad. Sci. USA* **103**, 10058–10063 (2006)
23. Navarrete, M., Araque, A.: Endocannabinoids mediate neuron-astrocyte communication. *Neuron* **57**, 883–893 (2008)
24. Nadkarni, S., Jung, P.: Dressed neurons: modeling neural-glia interactions. *Phys. Biol.* **1**, 35–41 (2004)
25. Nadkarni, S., Jung, P.: Modeling synaptic transmission of the tripartite synapse. *Phys. Biol.* **4**, 1–9 (2007)
26. Volman, V., Ben-Jacob, E., Levine, H.: The astrocyte as a gate keeper of synaptic information transfer. *Neural Comput.* **19**, 303–326 (2006)
27. Perea, G., Navarrete, M., Araque, A.: Tripartite synapses: astrocytes process and control synaptic information. *Trends Neurosci.* **32**, 421–431 (2009)
28. De Pittá, M., Volman, V., Berry, H., Ben-Jacob, E.: A tale of two stories: astrocyte regulation of synaptic depression and facilitation. *PLoS Comput. Biol.* **7**, e1002293 (2011). <https://doi.org/10.1371/journal.pcbi.1002293>
29. Postnov, D.E., Ryazanova, L.S., Sosnovtseva, O.V.: Functional modeling of neural-glia interaction. *Biosystems* **89**, 84–91 (2007)
30. Wade, J.J., McDaid, L.J., Harkin, J., Crunelli, V., Kelso, J.A.S.: Bidirectional coupling between astrocytes and neurons mediates learning and dynamic coordination in the brain: a multiple modeling approach. *PLoS ONE* **6**, e29445 (2011). <https://doi.org/10.1371/journal.pone.0029445>
31. Amiri, M., Bahrami, F., Janahmadi, M.: Functional contributions of astrocytes in synchronization of a neuronal network model. *J. Theor. Biol.* **292C**, 60–70 (2011)
32. Sasaki, T., Ishikawa, T., Abe, R., Nakayama, R., Asada, A., Matsuki, N., Ikegaya, Y.: Astrocyte calcium signalling orchestrates neuronal synchronization in organotypic hippocampal slices. *J. Physiol.* **592**(13), 2771–2783 (2014)
33. Pirttimäki, T.M., Sims, R.E., Saunders, G., Antonio, S.A., Codadu, N.K., Parri, H.R.: Astrocyte-mediated neuronal synchronization properties revealed by false gliotransmitter release. *J. Neurosci.* **37**(41), 9859–9870 (2017)
34. Szabó, Z., Héja, L., Szalay, G., Kékesi, O., Füredi, A., Szébenyi, K., Dobolyi, A., Orbán, T.L., Kolacsek, O., Tompa, T., Miskolczy, Z., Biczók, L., Rózsa, B., Sarkadi, B., Kardos, J.: Extensive astrocyte synchronization advances neuronal coupling in slow wave activity in vivo. *Sci. Rep.* **7**(1), 6018 (2017)
35. Poskanzer, K.E., Yuste, R.: Astrocytes regulate cortical state switching in vivo. *Proc. Natl. Acad. Sci.* **113**(19), E2675–E2684 (2016)
36. Lazarevich, I.A., Stasenko, S.V., Kazantsev, V.B.: Synaptic multistability and network synchronization induced by the neuron-glia interaction in the brain. *JETP Lett.* **105**(3), 210–213 (2017)
37. Gordleeva, S.Yu., Stasenko, S.V., Semyanov, A.V., Dityatev, A.E., Kazantsev, V.B.: Bi-directional astrocytic regulation of neuronal activity within a network. *Front. Comput. Neurosci.* **6**(92), 1–11 (2012)
38. Párpura, V., Zorec, R.: Gliotransmission: exocytotic release from astrocytes. *Brain Res. Rev.* **63**, 83–92 (2010)
39. Volterra, A., Meldolesi, J.: Astrocytes, from brain glue to communication elements: the revolution continues. *Nat. Rev. Neurosci.* **6**, 626–640 (2005)
40. Perea, G., Araque, A.: Astrocytes potentiate transmitter release at single hippocampal synapses. *Science* **317**, 1083–1086 (2007)
41. McGuinness, L., Taylor, C., Taylor, R.D.T., Yau, C., Langenhan, T., Hart, M.L., Christian, H., Tynan, P.W., Donnelly, P., Emptage, N.J.: Presynaptic NMDARs in the hippocampus facilitate transmitter release at theta frequency. *Neuron* **68**, 1109–1127 (2010)
42. Semyanov, A., Kullmann, D.M.: Modulation of GABAergic signaling among interneurons by metabotropic glutamate receptors. *Neuron* **25**, 663–672 (2000)
43. Henneberger, C., Papouin, T., Oliet, S., Rusakov, D.: Long-term potentiation depends on release of D-serine from astrocytes. *Nature* **463**, 232–236 (2010)
44. Bergersen, L.H., Morland, C., Ormel, L., Rinholm, J.E., Larsson, M., Wold, J.F., Roe, A.T., Stranna, A., Santello, M., Bouvier, D., Ottersen, O.P., Volterra, A., Gundersen, V.: Immunogold detection of L-glutamate and D-serine in small synaptic like microvesicles in adult hippocampal astrocytes. *Cereb. Cortex* **22**, 1690–1697 (2011)
45. Hodgkin, A.L., Huxley, A.F.: A quantitative description of membrane current and its application to conduction and excitation in nerve. *J. Physiol.* **117**, 500–544 (1952)
46. Shih, J.Y., Atencio, C.A., Schreiner, C.E.: Improved stimulus representation by short interspike intervals in primary auditory cortex. *J. Neurophysiol.* **105**(4), 1908–1917 (2011)
47. Martiniuc, A.V., Knoll, A.: Interspike interval based filtering of directional selective retinal ganglion cells spike trains. *Comput. Intell. Neurosci.* **2012**, 918030 (2012)
48. Abarbanel, H.D.I., Huerta, R., Rabinovich, M.I., Rulkov, N.F., Rovat, P.F., Selverston, A.I.: Synchronized action of synaptically coupled chaotic model neurons. *Neural Comput.* **8**, 1567–1602 (1996)
49. Zhou, C., Kurths, J.: Noise-induced synchronization and coherence resonance of a Hodgkin–Huxley model of thermally sensitive neurons. *Chaos* **13**, 401 (2003)

50. Ivanchenko, M.V., Osipov, G.V., Shalfeev, V.D., Kurths, J.: Phase synchronization in ensembles of bursting oscillators. *Phys. Rev. Lett.* **93**, 134101–4 (2004)
51. Wang, Q., Lu, Q., Chen, G., Guo, D.: Chaos synchronization of coupled neurons with gap junction. *Phys. Lett. A* **356**, 17 (2006)
52. Belykh, V.N., Pankratova, E.V.: Synchronization and control in ensembles of periodic and chaotic neuronal elements with time dependent coupling. *IFAC Proc. Vol.* **40**(14), 120–125 (2007)
53. Komarov, M.A., Osipov, G.V., Suykens, J.A.K.: Variety of synchronous regimes in neuronal ensembles. *Chaos* **18**, 037121 (2008)
54. Erichsen, R., Brunnet, L.G.: Multistability in networks of Hindmarsh-Rose neurons. *Phys. Rev. E* **78**(6), 061917 (2008)
55. Pankratova, E.V., Belykh, V.N., Mosekilde, E.: Dynamics and synchronization of noise perturbed ensembles of periodically activated neuron cells. *Int. J. Bifurc. Chaos* **18**(10), 2807–2815 (2008)
56. Wang, Z., Shi, X.: Lag synchronization of multiple identical Hindmarsh-Rose neuron models coupled in a ring structure. *Nonlinear Dyn.* **60**, 375–383 (2010)
57. Torres, J.J., Kappen, H.J.: Emerging phenomena in neural networks with dynamic synapses and their computational implications. *Front. Comput. Neurosci.* **7**, 30 (2013)
58. Ehrich, S., Pikovsky, A., Rosenblum, M.: From complete to modulated synchrony in networks of identical Hindmarsh-Rose neurons. *Eur. Phys. J. Spec. Topics* **222**, 2407–2416 (2013)
59. Araque, A., Navarrete, M.: Glial cells in neuronal network function. *Philos. Trans. R. Soc. Lond. B Biol. Sci.* **365**(1551), 2375–2381 (2010)
60. Syková, E., Nicholson, C.: Diffusion in brain extracellular space. *Physiol. Rev.* **88**, 1277–1340 (2008)
61. Theodosis, D.T., Poulain, D.A., Oliet, S.H.: Activity-dependent structural and functional plasticity of astrocyte-neuron interactions. *Physiol. Rev.* **88**, 983–1008 (2008)
62. Seifert, G., Schilling, K., Steinhäuser, C.: Astrocyte dysfunction in neurological disorders: a molecular perspective. *Nat. Rev. Neurosci.* **7**, 194–206 (2006)
63. Tzingounis, A.V., Wadiche, J.I.: Glutamate transporters: confining runaway excitation by shaping synaptic transmission. *Nat. Rev. Neurosci.* **8**, 935–947 (2007)
64. Maragakis, N.J., Rothstein, J.D.: Glutamate transporters: animal models to neurologic disease. *Neurobiol. Dis.* **15**, 461–473 (2004)

Publisher's Note Springer Nature remains neutral with regard to jurisdictional claims in published maps and institutional affiliations.